An Insect Vision-based Single-electron Circuit Performing Motion Detection

Andrew Kilinga Kikombo†, Tetsuya Asai and Yoshihito Amemiya

Graduate School of Science and Technology, Hokkaido University
Kita 14, Nishi 9, Kita-ku, Sapporo, 060-0814, Japan
Phone:+81-11-706-7149, Fax:+81-11-706-7890 † E-mail: kikombo@sapiens-ei.eng.hokudai.ac.jp

Abstract This paper proposes a bio-inspired single-electron circuit for detecting motion in projected images. Motion detection is a primary task performed in the retina as part of early vision processing. Based on a motion detection model, the correlation model ([4]), a number of motion detecting circuits have been proposed and implemented with CMOS mediums ([5], [6], [7], and others). In this paper, based on the same model, we propose a possible single-electron circuit configuration that can detect motion in incident images, and demonstrate its basic performance with a one-dimensional construction. Through Monte-Carlo based computer simulations, we confirmed that this construction can compute motion in projected images.

Keywords: Single-electron, Neuromophic circuits, Bio-inspired circuits, Beyond CMOS architectures.

1. Introduction

Nano-electronic devices are promising candidates for the next-generation of low-power LSIs and applications in parallel signal processing LSI systems [1]. So far several fabrication methodologies for single-electron devices have been proposed. As one of the Beyond CMOS candidates, single(few)-electron devices have been extensively studied, because they inherently operate with extreme low power dissipation and are thus viewed as promising functional devices for the next-generation of low-power LSI platforms. However, to apply these devices (which perform on new concepts in relation to the present conventional LSI devices) in functional circuits, we need to come up with new circuit architectures that (i) can accommodate their physical properties and high non-uniformity amongst individual devices (ii) fully utilize their high device density and (iii) provide a solution to their low-fault tolerance operation. One promising solution is to learn from living organisms, particularly insects, to create robust and highly effective signal processors—*neuromorphic-architectures* [2]. In this research, we propose an elementary image processor performing motion detection in incident images. The proposed circuit architecture is based on a widely studied neural correlation model [4].

In this work, toward realizing neuromorphic image processors with nano-electronic devices, we propose a basic circuit consisting of single-electronic devices and demonstrate that it can detect motion in incident images.

Motion detection is an essential task in first levels of visual information processing carried out in the retina. Living organisms, in particular insects, utilize motion detection to avoid collision and to navigate movements. Through hints from biological systems, we could create highly functional nano-electronic processors for special applications in parallel information processing. For the last two decades, electronic circuits based on how living organisms perform information processing—*neuromorphic engineering* ([2] - [3]) have been viewed as a breakthrough to creating highly parallel, real time information processors for the next generation of LSIs.

In this research, toward realising *neuromorphic* LSIs with nano-electronic devices, we propose a basic circuit consisting of single-electronic devices, which performs motion detection in incident images.

In the sections to follow, firstly, the model of motion detection in insects is illustrated, followed by a detailed explanation on LSI implementation of the model with single-electron devices. Finally, performance of the proposed circuit is evaluated through Monte-Carlo based computer simulations.

2. Motion detection scheme: The Correlation Model

The proposed circuit is based on the correlation motion scheme[4], one of the earliest biological motion detection systems based on the optomotor response of insects. In this model, motion detection is computed by comparing signals from a photoreceptor to delayed signals from adjacent photoreceptors. This is illustrated in Fig. 1(a). The photoreceptors (P_i) transduce light inputs (a light spot moving in the direction $\mathrm{P}_1 \rightarrow \mathrm{P}_2$ above the photoreceptors) in to electrical signals. The transduced signals are sent to both the corresponding correlators, and the neighboring pixels through delayers as shown in Fig. 1. For example, let's consider pixel 2. Photoreceptor P_2 receives light inputs to produce electrical signals corresponding to the light intensity. These signals are sent to the underlying correlator circuit C_2 and also to the adjacent correlator C_3 through delayer circuit d_2. Likewise, correlator C_2 receives a delayed signal from adjacent photoreceptor P_1 through d_1. Correlator C_2 gives an output, the product of these two signals (P_2 and d_1). In other words, C_2 calculates the correlation value between P_2 and d_1 signals. As illustrated in Fig. 1(b), and (c), if the two signals overlap, i.e., if the time the light spot takes to move from P1 to P2 ($\equiv t_{12}$) is equivalent to the delay time (τ), the correla-

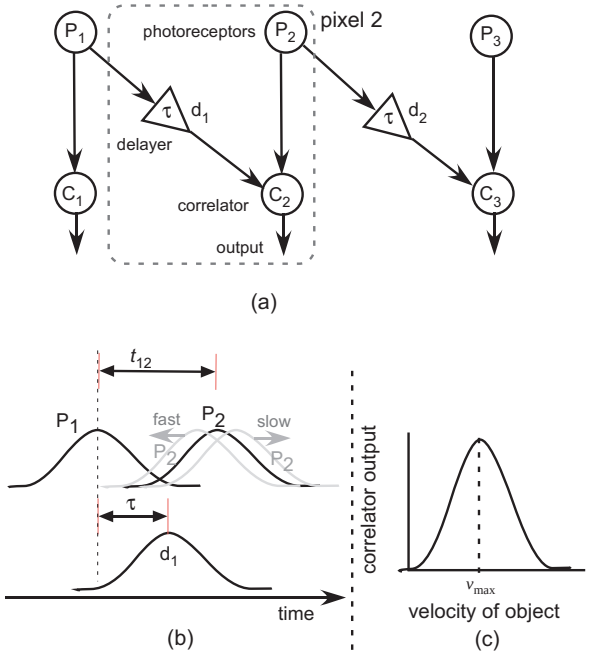

Fig. 1 Correlator model for motion detection: (a) configuration P: photoreceptor cells, d: delayers and c: correlators. (b),(c) Operation of the correlator model: (b) transient response of photoreceptors P_1, P_2 and delayer d_1. (c) Output (velocity response curve) of correlator C_2.

tor (C_2) gives the maximum output. This would be referred to as the maximum detectable velocity (v_{max}). Otherwise, if the velocity is lower (or higher) than the maximum velocity, the correlator gives a monotonously increasing (or decreasing) output (Fig. 1(c)).

3. Cicuit implementation

To implement the motion detection model, we employ local computations among single-electron oscillators. This section starts with a description of the conceptual circuit structure for implementing the motion detection model with single electron devices. Then the basic function of single-electron devices and details on implementation of the respective parts of the motion-detection model; the photoreceptor, delayer, and the correlator circuits are illustrated. Finally a unit pixel of the proposed motion detecting circuit is shown.

The conceptual schematic model circuit is shown in Fig. 2. It constitutes of photoreceptors $P_{i's}$, delayer circuits $D_{1,i's}$, interneuron circuits $I_{1,i's}$, and correlator circuits $C_{1,i's}$. Photoreceptor P_m receives light inputs to produce an excitatory signal toward correlator $C_{1,m}$. Similarly, photoreceptor P_k receives light inputs to produce excitatory signals toward the delayer circuit $D_{1,k}$. The delayer circuit in turn produces an

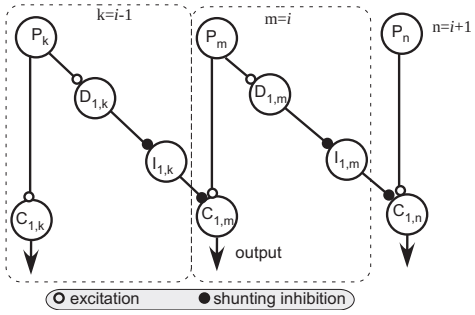

Fig. 2 Conceptual circuit configuration with single-electron devices. The photoreceptors ($P_{i's}$) receive light inputs to produce excitatory signals toward the delayer ($D_{1,i's}$) circuits. The delayer circuits in turn produce inhibitory signals toward interneurons ($I_{1,i's}$) which consequently send inhibitory signals toward correlator circuits ($C_{1,i's}$).

inhibitory signal toward interneuron $I_{1,k}$, which consequently produces an inhibitory signal toward the correlator $C_{1,m}$. The correlator calculates the correlation value of the two signals from neighboring photoreceptors; it gives a zero output at the maximum value of inhibitory signal $I_{1,k}$, or otherwise produces an increasing output as the magnitude of the inhibitory signal decreases.

Based on this basic configuration, the following subsections give details on how to realise the motion detecting circuit.

3.1. Single-electron oscillator

To realize the proposed motion detecting circuit, we employ single-electron oscillators. A single-electron oscillator consists of a tunneling junction C_j, resistance R and a bias voltage source (see insets in Fig. 3). When a positively-biased (or negatively-biased) oscillator is illuminated, photo-induced electron tunneling in C_j occurs [11] - [12], which leads to voltage drop (or increase) at the node (• in Fig. 3) because of electron tunneling from the ground (or node) to the node (or ground). To implement the motion detecting circuit, we utilize monostable single-electron oscillators.

3.2. Photoreceptor circuit

The retinal photoreceptor is implemented with a negatively biased single-electron oscillator. As explained in the previous subsection, in the absence of external interference, the photoreceptors assume a stable state where their node (nanodot) voltages take a value equivalent to the bias voltage. In the presence of light inputs (incoming photons), *photo-induced tunneling effect* ([11] - [12]) takes place inducing electron tunneling from the nanodot to the ground. This leads to a

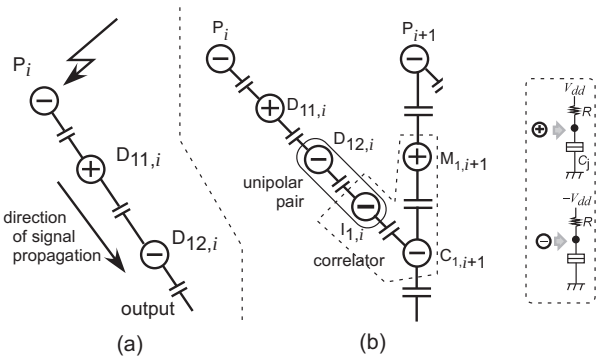

Fig. 3 (a) Delayer circuit: Signal propagation through oscillators in the delayer circuit. Photoreceptor (P_i) receives light inputs to produce an electrical signal, which is fed to underlying oscillator $D_{11,i}$ through a coupling capacitor. The signal is similarly relayed to oscillator $D_{12,i}$, (b) Signal propagation through delayer and correlator circuits.

jump in the node voltage from a low to a high value. We refer to this change as a firing event. The nanodot is recharged to its original stable state. The number of firing events would be proportional to the intensity of the illuminated light; low intensities would produce low firing rates and viceversa.

3.3. Delayer and Correlator circuits

The delayer circuit is realised through capacitively coupled single-electron oscillators, which form a delay transmission line [14]. This is illustrated in Fig. 3(a). Let's assume that photo-induced tunneling occurs at photoreceptor P_i. This triggers a signal flow toward underlying oscillators $D_{11,i}$ and $D_{12,i}$ as follows. Electron tunneling in P_i leads to a voltage increase in $D_{11,i}$ above its threshold, thus inducing it to tunnel. Likewise tuneling in $D_{11,i}$ reduces the node voltage of $D_{12,i}$ below the threshold value inducing it to tunnel [13] - [14]. Therefore signals emanating from the photoreceptors propagate through the series of positively and negatively biased oscillators (transmission line), with a time delay at each stage caused by stochastic nature of electron tunneling [8].

The basic circuit configuration of the conceptual circuit (Fig. 2) implemented with single-electron devices is shown in Fig. 3(b). Suppose a light spot is moving from from the left to the right. This triggers the photoreceptors to tunnel in turns, $P_i \rightarrow P_{i+1} \rightarrow \cdots$. The signals emanating from the photoreceptors are transmitted through the delayers as explained above. To implement the inhibition function between the delayer and correlator circuits, we introduce a unipolar pair in the trasmission line of positively- and negatively-biased oscillators. This is realised by introducing a capacitively coupled pair of negatively-biased oscillators between the delayer and the correlator circuit (see unipolar pair encircled with a solid line in Fig. 3(b)). Therefore signals flowing from the delayer circuit raise the node voltages of the unipolar pair, and consequently the correlator terminal circuit ($C_{1,i+1}$), thus inhibiting them from tunneling, even in the presence of an external trigger input. On the other hand, tunneling in P_{i+1} induces tunneling in $M_{1,i+1}$, which in turn induces $C_{1,i+1}$ to tunnel. The correlator circuit, $C_{1,i+1}$, receives excitatory signals from $M_{1,i+1}$ and inhibitory signals from $I_{1,i}$ (with which it makes a unipolar pair). Thus the tunneling rate of $C_{1,i+1}$ remains at a low value (almost zero) as inhibitory signals are fed from the delayer circuit ($D_{13,i}$), and increases as the inhibition signal decays with time.

3.4. Unit pixel circuit

A unit pixel of the motion detecting circuit is shown in Fig. 4. This configuration can only detect motion in images (light spots) travelling from the left toward the right. A circuit configuration for detecting bi-directional motion is illustrated in Fig. 5(a). The subscript "1" (for open circles) denotes circuits responsible for left-right motion detection, while "2" (for shaded circles) shows circuits responsible for right-left motion detection. The correlation value in both directions is produced at the coresponding correlators $C_{1,n}$ and $C_{2,n}$ (for the $i_{\rm th}$ pixel) for left-right and right-left motions respectively. These signals are fed to the underlying layer (see dotted box in Fig. 5(a)) where the final correlation value, and hence motion velocity is determined. The circuit configuration of a unit pixel of the dotted region is shown in Fig. 5(b). Let's assume the light spot is moving from the left to the right. The correlator circuit ($C_{1,i}$) would produce a signal corresponding to the velocity of the light spot as explained above. Note that as the light spot moves to the right, the magnitude of the inhibition signal toward the "left" direction correlator circuit remains high, as opposed to decreasing inhibition signal sent to the "right" direction correlator circuit, as explained in Section 3.3. Therefore, for images travelling fom the left to the right, the correlator circuit $C_{2,i's}$ would produce a zero output in comparison to correlator $C_{1,i}$. The signals from correlator $C_{1,i}$ are fed to C_i through the right branch via oscillator $O_{1,i}$. At the same time, $C_{1,i}$ sends inhibitory signals to the left branch (toward $O_{2,i}$), blocking any signals from the $C_{2,i}$ oscillator. The same is repeated in a leftward motion detection. Therefore, this mechanism makes it possible to detect motion in both directions and to produce an output value of zero at C_i for stationary images.

4. Simulation results

The operation of the proposed motion detection circuit was investigated with a one-dimensional array construction consisting of 100 unit pixels. A unit pixel is shown in Fig. 5 (unit pixel). Light inputs were simulated with an external trigger

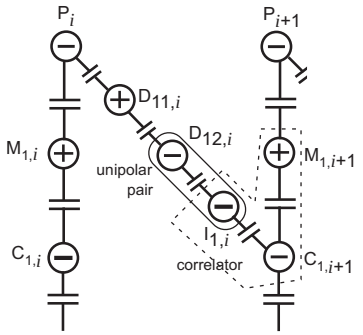

Fig. 4 Unit pixel configuration of the motion detecting circuit for left $\rightarrow$ right images.

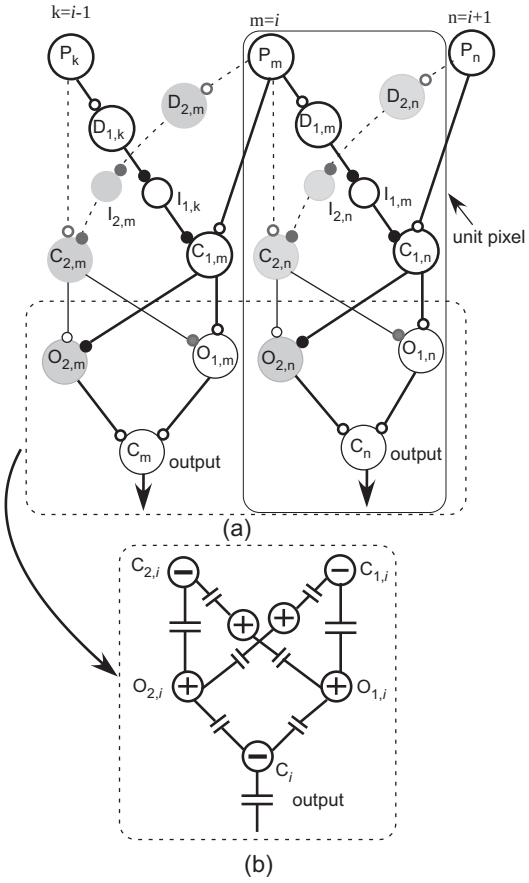

Fig. 5 (a) Conceptual circuit configuration for bi-directional motion detection. Open circles denoted with subscript $(1,i)$ represent circuits responsible for left $\rightarrow$ right motion detection, while shaded circles denoted with subscript $(2,i)$ represent delayer, interneural and correlator circuits responsible for motion detection in images moving from the right toward the left. (b) Circuit configuration of the overall correlation circuit (dotted portion in (a)) of the bi-directional motion detector.

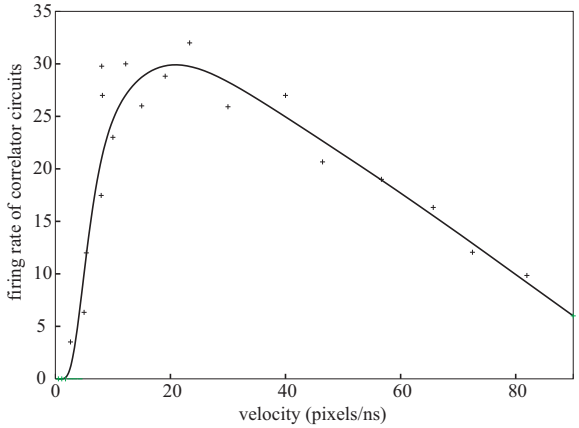

Fig. 6 Motion detection with a 100 pixel array construction. Vertical axis shows the maximum firing rate of the $50th$ correlator circuit against the projected image velocity. Simulated with images moving from the left to the right at zero temperature. Maximum frequency of input trigger is set to 50 MHz.

input whose frequency is equivalent to the intensity of the input light. The trigger input was set to an amplitude of 2.5 mV and the light intensity was simulated with a maximum frequency of 50 MHz. All excitatory and inhibitory capacitive couplings were implemented with a capacitance (C) of 2 aF, whereas tunneling junction capacitance C_j was set to 10 aF.

4.1. Velocity response curve

With the above construction, we investigated the response of the proposed motion detector to images (light spots) travelling at different velocities, to obtain the velocity response curve. The velocity response curve (VRC) was obtained by plotting the maximum firing rate of correlator circuits against the velocity of projected images. Fig. 6 shows the VRC of the $50th$ correlator circuit as a function of the projected image velocity moving from the left toward the right at zero temperature. The proposed circuit can detect motion in projected images with a maximum detectable velocity of 20 pixels/ns. This would correspond to a maximum velocity of 2 Km/s if adjacent photoreceptors were fabricated at a pitch of 100 nm. The maximum detectable velocity can be tuned by adjusting the delay-time τ along the transmission line. This can be achieved by increasing (or decreasing) the number of oscillators along the transmission line to increase (or decrease) the maximum detectable velocity.

4.2. Response to light intensity

As mentioned in subsection 3.2, the firing rate of the photoreceptor circuits is proportional to the light intensity. To confirm the response of the proposed circuit to light inten-

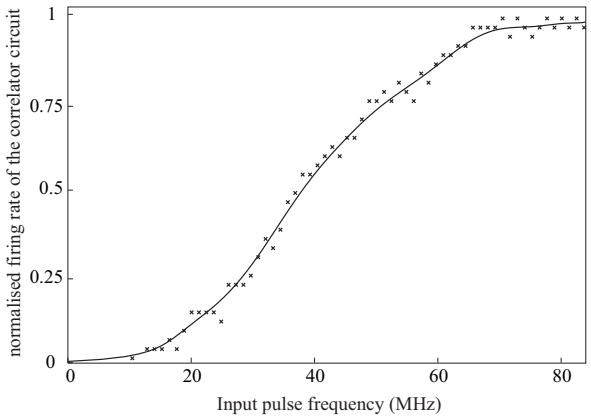

Fig. 7 Response to light intensity simulated by varying the maximum frequency of input tigger signal. Vertical axis represents the maximum firing rate of the 50*th* correlator circuit, normalised with the maximum firing rate at 75 MHz. Simulated at zero temperature.

sity, images with different light intensities (and constant velocity) were projected onto the 100-pixel retinomorphic circuit. Fig. 7 shows the response of the 50*th* correlator circuit to various light intensities, for images travelling at a constant velocity of 20 pixels/ns. The vertical axis shows the maximum output of the 50*th* correlator circuit at zero temperature. The firing rate of the correlator circuit (output) increases with increase in light intensity to attain a maximum value at a light intensity of 75 MHz. The vertical axis is normalised with the firing rate at 75 MHz.

4.3. Temperature characteristics

We evaluated the temperature performance of the motion detecting circuit with increasing temperatures by plotting the *hump* (see Fig. 8(a)) height against the temperature. The *hump* height is the difference between the firing rate at zero velocity and at the maximum detectable velocity. We refer to this as the signal-noise (SN) ratio. We observed that as the temperature increases, random firing as a result of thermal induced electron tunneling within the circuit also increases (Fig. 8(a), (b), and (c) simulated at T = 5, 10, and 20 K respectively). As a result the height of the hump (SN ratio) decreases, and finally flattens at high temperatures. Fig. 9 shows the simulated results for a temperature range between 0 and 30 K. The vertical axis, *hump* height is normalized with the maximum height at zero temperature. With the present configuration, the proposed circuit can perform at signal-noise ratio of 0.4 at 20 K.

5. Summary

We proposed a motion detection circuit based on corre-

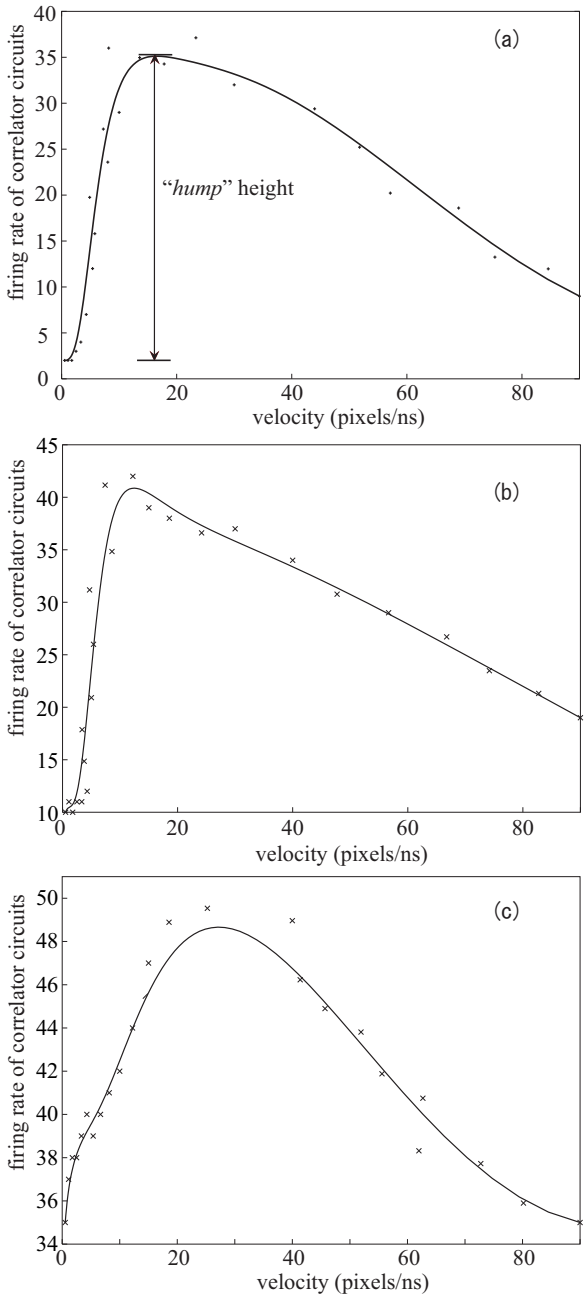

Fig. 8 Velocity response curves simulated for temperature T = 5 K (a), 10 K (b), and 20 K (c). Vertical axis shows the maximum firing rate of the 50*th* correlator circuit against the projected image velocity.

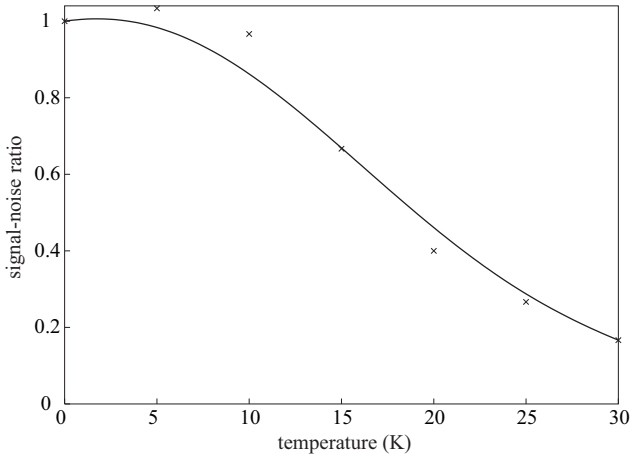

Fig. 9 Temperature characterists: *hump* height (signal-noise ratio) plotted against temperature. Vertical axis is normalised with the SN ratio at zero temperature.

lation neural models in insects. Based on this model, we proposed a circuit structure with single-electron devices and evaluated its peformance through Monte-carlo based simulations. The proposed circuit could detect motion in images with a maximum detectable velocity of 20 pixels/ns. The temperature characteristics of the proposed circuit were analysed. The circuit could detect motion in images with a signal-noise ratio of 0.4 at 20 K.

References

[1] S. Bandyopadhyay and V. Roychowdhury, "Computational paradigms in nano-electronics: quantum coupled single electron logic and neuromorphic networks", *Jpn. J. Appl. Phys.*, vol. 35, pp. 3350-3362, **1996**.

[2] Carver Mead, Analog VLSI and Neural Systems, Addison-Wesley (**1989**).

[3] R. Douglas, M. Mahowald, and C. Mead, *Annual Review of Neuroscience*, 18, 255 (**1995**).

[4] W. Reichard, Autocorrrelation, a principal for the evaluation of sensory information by the central nervous systems, in: Sensory communication, Contributions to the Symposium on Principles of Sensory Communication, edited by W.A. Rosenblith, MIT Press, (**1961**), pp. 303-317.

[5] T. Delbrück, "Silicon retina with correlation-based, velocity-tuned pixels," *IEEE Trans. Neural Networks*, 4, 521 (**1993**).

[6] A. Moini, A. Bouzerdoum, K. Eshraghian, A. Yakovleff, X.T Nguyen A. Blanksby, R. Beare, D. Abbott, and R.E. Bonger, "An insect vision-based motion detection chip," *IEEE J. Solid State Circuits*, 32, 279 (**1997**).

[7] T. Asai, M. Ohtani, H. Yonezu, "Analog MOS circuits for motion detection based on corrrelation neural networks," *Jpn. J. Appl. Phys.*, 38, 2256 (**1999**).

[8] H. Gravert and M.H. Devoret, Single Charge Tunneling—Coulomb Blockade Phenomena in Nanostructures, New York: Plenum, (**1992**).

[9] K.K. Likharev and A.B. Zorin , "Theory of the Bloch-wave oscillations in small Josephson junctions," *J. of Low Temp. Phys.*, 59, 347 (**1985**).

[10] D.V. Averin and K.K. Likharev "Coulomb blockade of single-electron tunneling, and coherent oscillations in small tunnel junctions," *J. of Low Temp. Phys.*, 62, 345 (**1986**).

[11] A. Fujiwara, Y. Takahashi, and K. Murase, "Observation of single electron-hole recombination and photon-pumped current in an asymmetric Si single-electron transistor," *Phys. Rev. Lett.*, 78, 1532 (**1997**).

[12] R. Nuryadi, Y. Ishikawa, and M. Tabe, "Single-photon-induced random telegraph signal in a two-dimensional multiple-tunnel-junction array," *Phys. Rev. B*, 73, 45310 (**2006**).

[13] T. Oya, T. Asai, T. Fukui, and Y. Amemiya, "Reaction-Diffusion Systems Consisting of Single-Electron Oscillators, *Int. J. Unconventional Computing*, 1, 177 (**2005**).

[14] T. Oya T., A. Schmid, T. Asai, Y. Leblebici, and Y. Amemiya, "On the fault tolerance of a clustered single-electron neural network for differential enhancement," *IEICE Electronics Express*, 2, 76 (**2005**).